BMB
reports

HP0902 from *Helicobacter pylori* is a thermostable, dimeric protein belonging to an all-β topology of the cupin superfamily

Dae-Won Sim[1], Yoo-Sup Lee[1], Ji-Hun Kim[2], Min-Duk Seo[2], Bong-Jin Lee[2] & Hyung-Sik Won[1,]*

[1]Department of Biotechnology, College of Biomedical and Health Science, Konkuk University, Chungju, 380-701, [2]Reseearch Institute of Pharmaceutical Sciences, College of Pharmacy, Seoul National University, Seoul 151-742, Korea

Here, we report the first biochemical and structural characterization of the hypothetical protein HP0902 from *Helicobacter pylori*, in terms of structural genomics. Gel-permeation chromatography and dynamic light scattering indicated that the protein behaves as a dimer in solution. Circular dichroism spectroscopy showed that HP0902 primarily adopts a β-structure and the protein was highly thermostable with a denaturing temperature higher than 70°C. Finally, the backbone NMR assignments were obtained on the [^{13}C,^{15}N]HP0902 and the secondary structure was determined using the chemical shift data. Additionally, the local flexibility was assessed via a heteronuclear ^{1}H-^{15}N steady state NOE experiment. The results revealed that HP0902 would adopt a compactly folded, all-β topology with 11 β-strands. All of the results clearly support the notion that HP0902 belongs to the cupin superfamily of proteins. [BMB reports 2009; 42(6): 387-392]

INTRODUCTION

As an area of extensive research in the postgenomic era, structural genomics (also known as structural proteomics) projects are being conducted worldwide and expending great efforts toward expanding knowledge of the protein universe (1-3). Basically, structural genomics aims to understand the relationship between protein sequence, structure, and function, by determining the structure of uncharacterized gene products (4). Through the rapid progress of structural genomics, a vast number of structures have been recently determined for hypothetical proteins identified by genome projects (5). By proposing molecular and cellular functions for unannotated proteins, structural genomics studies of human pathogens have been useful in identifying potential drug targets and in providing critical information for structure-based drug discovery (6-10). In particular, NMR spectroscopy has been employed efficiently for both structural genomics (11-13) and structure-based drug discovery efforts (14-17), by monitoring protein structures in a solution state. In this work, as a component of our structural genomics examinations of the human gastric pathogen *Helicobacter pylori,* the hypothetical protein HP0902 (UniProtKB/TrEMBL ID O25562) was investigated via NMR.

Helicobacter pylori, infection with which can induce severe gastric disorders including chronic gastritis, peptic ulcers, and stomach cancer (18, 19), is known to colonize the stomach in approximately half of the human population (20). Owing to its importance as a human pathogen, the genome of *H. pylori* has been sequenced completely for three strains: 26695, J99, and HPAG1 (21-23). According to the JCVI CMR database (http://cmr.jcvi.org/tigr-scripts/CMR/CmrHomePage.cgi), a total of 1,587, 1,712, and 1,610 genes are identified as protein coding genes, respectively, in the strains 26695, J99 and HPAG1, including hypothetical genes (470 genes for the 26,695, 180 for the J99, and 113 for the HPAG1) and conserved hypothetical genes (184 genes for the 26,695, 358 for the J99, and 318 for the HPAG1). Subsequently, structural genomics studies on *H. pylori* are currently being attempted by several groups around the world (24-28). Structural information on the hypothetical proteins from *H. pylori* would facilitate the selection of drug targets.

In particular, HP0902 from *H. pylori* 26,695 may be an important virulence factor, for the following reasons. As the secretion of proteins by *H. pylori* may contribute to gastric inflammation and epithelial damage, a recent study by Kim *et al*. (29) has searched for proteins released by *H. pylori in vitro*. The HP0902 protein was identified as one of the 13 proteins that are probably secreted by *H. pylori*. In another study, HP0902 was identified as one of the over-expressed proteins in a mutant strain of *H. pylori* lacking the *fdx*A gene, which regulates the resistance of *H. pylori* to the antibiotic metronidazole (30, 31). Thus, we expect that our structural genomics study on HP0902 would ultimately facilitate the functional identification of the protein, thereby contributing to the understanding of the mechanisms underlying the pathogenicity and resistance behaviors of *H. pylori*. As an initial step, the molecular organization, thermostability, and structural topology of HP0902 were addressed in this study. The results constitute the first biochemical and structural characterization of this protein.

*Corresponding author. Tel: 82-43-840-3589; Fax: 82-43-852-3616; E-mail: wonhs@kku.ac.kr

Received 21 January 2009, Accepted 28 January 2009

Keywords: All-β topology, Cupin superfamily, *Helicobacter pylori*, HP0902, NMR spectroscopy, Secondary structure

RESULTS AND DISCUSSION

Biochemical characterization

The isoelectric point of HP0902 was predicted as 6.19, according to sequence analysis conducted with the ProtParam tool of the ExPASy Proteomics Server (http://www.expasy.org). Anion exchange chromatography proved efficient in the purification of HP0902, due to its acidic properties. The purified HP0902 was readily precipitated in a time-dependent manner at relatively higher (more than submillimolar) concentrations. This unfavorable aggregation tendency could be overcome via the addition of the reducing agent DTT in the protein solution, whereas the precipitation was accelerated via the addition of a small aliquot of the oxidant hydrogen peroxide. Thus, one or both of two cysteines in HP0902 were suggested to be exposed to the surface of the protein, thereby forming unfavorable disulfide bonds which result in the precipitation of the protein at high concentrations. The exact protein concentration could not be estimated spectrophotometrically, as HP0902 possesses neither tryptophan nor tyrosine residues. Thus, a typical Bradford method or a BCA method was employed in order to measure the protein concentration. Although the results by the two different methods were similar, the determined concentration could not be quantitatively ensured. For example, the signal intensities in the following CD and NMR spectra were substantially stronger than those generally expected for the determined concentration.

The molecular weight of HP0902 was calculated as 11.03 kDa from the protein sequence. However, in our initial NMR approach on a 500 MHz machine equipped with a cryoprobe, the spectral quality of HP0902 was relatively poor with a severe line broadening, which would be expected from a higher molecular weight system. Thus, the molecular organization was explored via gel-permeation chromatography. As is shown in Fig. 1, the apparent molecular weight of HP0902 was determined to be approximately 26 kDa, thus suggesting a dimeric organization of the protein. In support of this notion, DLS analysis also indicated a major species of 23 kDa protein in the purified HP0902 solution. Thus, HP0902 could be concluded to be a dimeric protein with a molecular weight of 22.1 kDa, and the suitable quality of the NMR spectra could be ultimately obtained via measurement in a TROSY-type, on a higher field (800 MHz) machine, and at a high temperature (40°C). The thermal stability of HP0902 was evaluated by a temperature scan of CD signals (Fig. 2). The results demonstrated that HP0902 is highly thermostable. The protein was not denatured until 65°C and the apparent melting point was approximately 71.5°C.

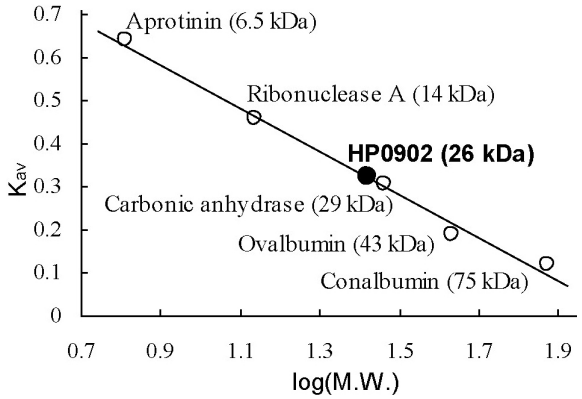

Fig. 1. Apparent molecular weight of HP0902, as estimated by gel-permeation chromatography analysis. Open circles indicate the protein standards used. Filled circle designates the K_{av} value of HP0902, of which molecular weight was calculated using the standard curve.

Structural characterization

The conformational preference of HP0902 was assessed via CD spectroscopy. The far-UV CD spectrum (inset in Fig. 2) implied that the protein primarily adopts a β-structure, evidencing a single negative minimum at 216 nm. In an effort to acquire more detailed information regarding the secondary structure, heteronuclear multidimensional NMR experiments were conducted on the [^{13}C, ^{15}N]HP0902. On the basis of a series of triple resonance spectra, the backbone $^{1}H^{N}$ and ^{15}N resonances in the 2D-TROSY spectrum could be completely assigned (Fig. 3). However, NMR signals from H5, G9, F12, L15, S24, G62, and D63 were not detected in the spectrum. Thus, they appear to have undergone an intermediate rate of chemical exchange in the NMR time scale. As the majority of the missing signals were assigned to the loop regions in the secondary structure (Fig. 4), the possibility of dynamic conformational equilibrium in the corresponding sites cannot be dismissed. Additionally, the complete assignments of the 2D-

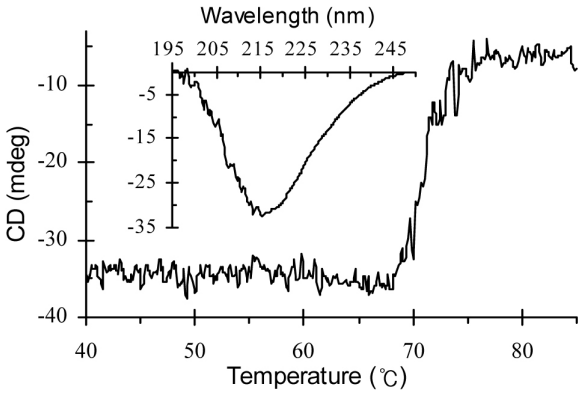

Fig. 2. Conformational preference and thermal stability of HP0902, as evaluated by CD spectroscopy. The protein concentration was approximately 4 μM, as estimated by typical Bradford and BCA assays (refer to the text for other experimental details). Inset shows the far-UV CD spectrum of the protein at 20°C. Since the negative minimum was observed at 216 nm, thermal denaturation was monitored at the wavelength.

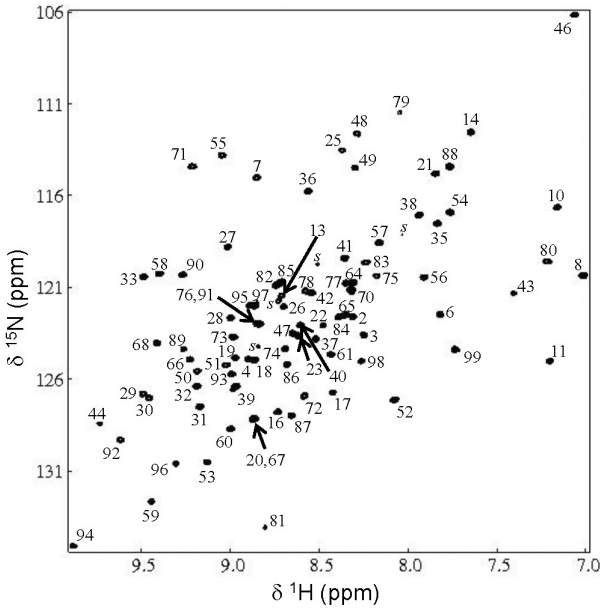

Fig. 3. NMR assignments of the [^{13}C, ^{15}N]HP0902, indicated on the 2D-TROSY spectrum. The amide signals from Asn and Gln side-chains were technically suppressed and other side-chain signals (probably from arginines) are marked with "*s*". The other peaks from backbone amides are marked with the corresponding residue numbers (refer to Fig. 4 for the amino acid sequence).

TROSY spectrum without doubling of peaks supported the notion that HP0902 formed a symmetric dimer in solution.

Despite the missing resonances of amide $^{1}H^{N}$ and ^{15}N, the other nuclei ($^{13}C^{\alpha}$, $^{13}C^{\beta}$, and $^{13}C{=}O$) could be nearly completely assigned by the inter-residue ^{13}C correlation in the triple resonance spectra; only the G62 residue could not be assigned, owing to a break in sequential connectivity. Finally, the secondary structure of HP0902 was determined using the ^{13}C chemical shift data (Fig. 4). Both the CSI and the TALOS results on the ^{13}C chemical shifts were indicative of an overall tendency toward a β-structure, which was consistent with the CD results. By combining the CSI and the TALOS prediction, no helical segment was supported, but 11 β-strands were evident in the HP0902 structure: residues M1-V4, V10-F12, H16-E18, H26-I31, A37-A44, I48-Q51, K56-V61, K65-P69, A72-L76, R83-D85, and E88-L94. The tertiary structure of HP0902 appears to be compactly folded. In the heteronuclear ^{1}H-^{15}N NOE experiments (Fig. 4), neither negative nor zero NOEs were detected, even for the terminal residues. The majority of residues, including most of the loop regions, evidenced positive NOE values of higher than 0.7, thereby indicating a significant rigidity.

Database search

HP0902 is categorized in the JCVI CMR database into a hypothetical protein with no predicted transmembrane motif.

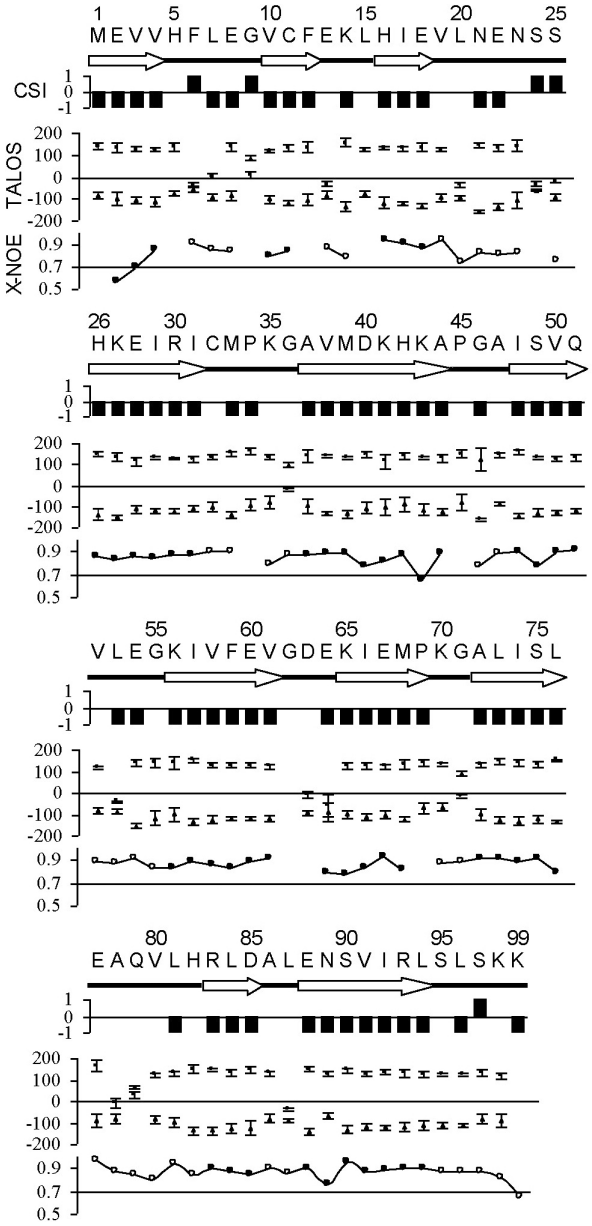

Fig. 4. Secondary structure and local flexibility of HP0902. The CSI results are depicted as a consensus-CSI ("1" for α-helix and "-1" for β-strand tendency), which were derived by a simple "majority rule" (two or three out of three) from the individual CSI of each ^{13}C atom ($^{13}C^{\alpha}$, $^{13}C^{\beta}$, and ^{13}C = O). The TALOS results show the predicted backbone dihedral ϕ (triangles) and φ (circles) angles with the standard deviation (error bars). The secondary structure element was defined at the region where three or more consecutive residues evidence the same secondary structure preference seen in both the CSI and TALOS results. The determined secondary structure is displayed with the arrows for β-strands along the sequence. The β-strand regions in the heteronuclear ^{1}H-^{15}N NOEs (X-NOEs) are shown as filled circles.

Although no paralogue protein was detected in the same strain, the database reports total 20 proteins from other species with more than 30% of sequence homology to HP0902. However, none of them has yet been characterized in terms of structure or function. In the Pfam database (http://pfam.sanger.ac.uk/), HP0902 is classified as a member of the cupin superfamily (32-34). The term cupin originates from the Latin term *cupa* for a small barrel, and thus describes a conserved β-barrel fold. The protein superfamily was originally discovered in plants, but is now divided in the Pfam database into 24 subfamilies from diverse species, including many bacteria. Many proteins in the cupin superfamily have been shown to be unusually thermostable and some subfamilies require certain metal ions to function (32-34). As the cupin superfamily is one of the most functionally diverse groups of proteins, the manner in which such a well-conserved cupin structure can encompass so many different biochemical functions remains an intriguing issue. We found approximately 80 structures recognized as cupin family proteins in the Protein Data Bank (PDB, http://www.rcsb.org/pdb/home/home.do). Thus, we searched the PDB for structures with significant sequence homology to HP0902 and identified a tetrameric protein (PDB code 3FJS) and a monomeric protein (PDB code 1YHF). Both of them belonged to the cupin superfamily, originating from bacterial sources, with similar polypeptide lengths (114 and 115 residues, respectively) with that of HP0902. Although the two proteins both harbor an β-helix in their N-terminal regions, they were well-matched with HP0902, even at the level of secondary structure assessed in the present study. Unfortunately, however, both the 1YHF and 3FJS proteins remain functionally uncharacterized.

Concluding remarks

The present results constitute the first biochemical and structural characterization of the hypothetical protein HP0902 from *H. pylori*. HP0902 consists of 99 amino acid residues, but the results of the present study suggest a dimeric organization that leads to a molecular weight of 22.1 kDa. On the basis of the JCVI CMR database, 2 β-helices and 5 β-strands were predicted from the protein sequence, but the present results showed an all-β topology with 11 β-strands. In addition to the primary and secondary structures, the high thermostability supported the notion that HP0902 belongs to the cupin superfamily of proteins. According to the present results, the following two subjects can be raised for a future direction of investigation to infer a plausible function and functional mechanism of HP0902: 3D structure and metal-binding properties. These progressive researches in our laboratory would enable us to design appropriate functional assays for the final identification of the precise function of HP0902 in the pathogen *H. pylori*. Additionally, we expect that the present results will eventually provide the most fundamental and critical data for progressing studies of 3D structure and intermolecular interaction with substrates and other proteins.

MATERIALS AND METHODS

DNA constructs and protein preparation

In order to generate a recombinant protein, the ORF of HP0902 was PCR-amplified using genomic DNA from *H. pylori* (ATCC 700392) as a template, as well as the appropriate primers containing restriction sites. The PCR products were digested with *Nde*I and *Xho*I and subsequently ligated into the pET-15b vector, yielding an N-terminally 6-histidine-tagged protein (H_6HP0902). The constructed plasmid was then confirmed via DNA sequencing and transformed into *E. coli* BL21(DE3)pLysS. The cells were grown in M9 minimal medium at 37°C and protein expression was induced by adding IPTG. To prepare an isotope-enriched protein ([^{13}C,^{15}N] HP0902) for NMR, the M9 medium was supplemented with [^{13}C]glucose and [^{15}N]NH_4Cl as the sole source of carbon and nitrogen. The harvested cells were then disrupted by sonication, and from the supernatant, the H_6HP0902 was purified via sequential chromatography on a nickel-affinity column and an anion-exchange column. The tagged histidines were then cleaved with thrombin, followed by the removal of thrombin and other impurities via the sequential application of nickel-affinity, anion-exchange, and gel-permeation chromatography. Finally, the purified solution was concentrated and buffer-exchanged by ultrafiltration (Amicon). For all other experiments, a standard buffer of 20 mM Tris-HCl containing 150 mM NaCl, 2 mM DTT, and 1 mM EDTA, at pH 7.8, was employed as a solvent. Protein concentration was estimated as a monomer, via typical Bradford and BCA assays.

Gel-permeation chromatography

Purified HP0902 and molecular weight standards (Pharmacia) were applied on a HiLoad 16/60 Superdex^{TM} 75 (Pharmacia) gel-permeation column with a total bed volume (v_t) of 120 ml. The column was preequilibrated with the standard buffer and run at a 1 ml/min flow rate. The column void volume (v_o) was determined as the elution volume for Blue Dextran 2000. From the elution volume (v_e) of each sample, the gel-phase distribution coefficient (K_{av}) was calculated using the equation: $K_{av} = (v_e-v_o)/(v_t-v_o)$. The standard curve was generated by plotting K_{av} against the logarithm of molecular weight, for standard proteins (35). By fitting the K_{av} of HP0902 into the standard curve, its apparent molecular weight was estimated.

DLS and CD spectroscopy

The dynamic light scattering data were collected on a Viscotek DLS 802 Detector at room temperature and analyzed automatically using the OmniSize^{TM} software supplied by the manufacturer. CD measurements were conducted on a Jasco J-715 spectropolarimeter equipped with a temperature-controlling unit, using a 0.2 cm path-length cell, with a bandwidth of 1 nm and a response time of 4 s. For the far-UV CD spectrum, three individual scans taken from 260 to 190 nm at 20°C

were summed and averaged, followed by the subtraction of the solvent CD signal. To monitor thermal denaturation, CD signals at 216 nm were recorded every 0.1°C, with increasing temperature from 20°C to 90°C at a rate of 1°C/min. The half-denaturing temperature (melting point, T_m) was determined as previously described (35-37).

NMR[#] spectroscopy

NMR spectra were acquired on a Bruker Biospin Avance 800 spectrometer at 313 K, processed using the NMRPipe/NMRDraw software (38), and analyzed with NMRView software (39). Chemical shifts were referenced directly to DSS for the ^{1}H and ^{13}C atoms and indirectly for the ^{15}N, using the chemical shift ratio value suggested in the BMRB (http://www.bmrb.wisc.edu). 2D-TROSY and the following TROSY-based triple resonance spectra were recorded on the [^{13}C, ^{15}N]HP0902 (approximately 0.5 mM, estimated by Bradford and BCA assays): HNCACB, HN(CO)CACB, HNCO, and HN(CA)CO. Sequential assignments were achieved via the verification and linkage of peak clusters, as illustrated previously (40, 41). To determine the secondary structure, CSI and TALOS analyses were conducted on the assigned ^{13}C chemical shifts, as demonstrated previously (42). The ^{1}H-^{15}N steady-state heteronuclear NOE values were determined from the spectra recorded with (NOE experiment) and without (NONOE) experiment) a proton presaturation period of 3 s, also as previously described (42).

Footnotes to the text

[#]For NMR experiments, this study made use of the NMR facility at the Korea Basic Science Institute, which is supported by the Bio-MR Research Program of the Korean Ministry of Science and Technology (E28070).

Acknowledgements

This work was supported by the Regional Innovation Center Program of the Ministry of Commerce, Industry and Energy through the Bio-Food & Drug Research Center at Konkuk University, Korea. The authors thank Drs. Young-Ho Jeon, Kyoung-Seok Ryu and specially Eun-Hee Kim at the Korea Basic Science Institute (http://www.amrb.kbsi.re.kr) for their generous support of the use of the DLS detector and for the help for NMR operation.

REFERENCES

1. Grabowski, M., Joachimiak, A., Otwinowski, Z. and Minor, W. (2007) Structural genomics: keeping up with expanding knowledge of the protein universe. *Curr. Opin. Struct. Biol.* **17,** 347-353.
2. Rigden, D. J. (2006) Understanding the cell in terms of structure and function: insights from structural genomics. *Curr. Opin. Biotechnol.* **17,** 457-464.
3. Blow, N. (2008) Structural genomics: inside a protein structure initiative center. *Nat. Methods* **5,** 203-207.
4. Marsden, R. L. and Orengo, C. A. (2008) Target selection for structural genomics: an overview. *Methods Mol. Biol.* **426,** 3-25.
5. Berman, H. M. and Westbrook, J. D. (2004) The impact of structural genomics on the protein data bank. *Am. J. Pharmacogenomics* **4,** 247-252.
6. Weight, J., McBroom-Cerajewski, L. D., Schapira, M., Zhao, Y. and Arrowmsmith, C. H. (2008) Structural genomics and drug discovery: all in the family. *Curr. Opin. Chem. Biol.* **12,** 32-39.
7. Lundstrom, K. (2006) Structural genomics: the ultimate approach for rational drug design. *Mol. Biotechnol.* **34,** 205-212.
8. Baker, E. N. (2007) Structural genomics as an approach towards understanding the biology of tuberculosis. *J. Struct. Funct. Genomics* **8,** 57-65.
9. Fan, E., Baker, D., Fields, S., Gelb, M. H., Buckner, F. S., Van Voorhis, W. C., Phizicky, E., Dumont, M., Mehlin, C., Grayhack, E., Sullivan, M., Verlinde, C., Detitta, G., Meldrum, D. R., Merritt, E. A., Earnest, T., Soltis, M., Zucker, F., Myler, P. J., Schoenfeld, L., Kim, D., Worthey, L., Lacount, D., Vignali, M., Li, J., Mondal, S., Massey, A., Carroll, B., Gulde, S., Luft, J., Desoto, L., Holl, M., Caruthers, J., Bosch, J., Robien, M., Arakaki, T., Holmes, M., Le-Trong, I. and Hol, W. G. (2008) Structural genomics of pathogenic protozoa: an overview. *Methods Mol. Biol.* **426,** 497-513.
10. Frishman, D. (2003) What we have learned about prokaryotes from structural genomics. *OMICS* **7,** 211-224.
11. Yee, A., Gutmanas, A. and Arrowsmith, C. H. (2006) Solution NMR in structural genomics. *Curr. Opin. Struct. Biol.* **5,** 611-617.
12. Shin, J., Lee, W. and Lee, W. (2008) Structural proteomics by NMR spectroscopy. *Expert Rev. Proteomics* **5,** 589-601.
13. Sue, S.-C., Chang, C.-F., Huang, Y.-T., Chou, C.-Y. and Huang, T.-H. (2005) Challenges in NMR-based structural genomics. *Physica. A* **350,** 12-27.
14. Powers, R., Mercier, K. A. and Copeland, J. C. (2008) The application of FAST-NMR for the identification of novel drug discovery targets. *Drug Discov. Today* **13,** 172-179.
15. Wishart, D. (2005) NMR spectroscopy and protein structure determination: applications to drug discovery and development. *Curr. Pharm. Biotechnol.* **2,** 105-120.
16. Homans, S. W. (2004) NMR spectroscopy tools for structure-aided drug design. *Angew. Chem. Int. Ed. Engl.* **43,** 290-300.
17. Pellecchia, M., Sem, D. S. and Wüthrich, K. (2002) NMR in drug discovery. *Nat. Rev. Drug Discov.* **3,** 211-219.
18. Ferreira, A. C., Isomoto, H., Moriyama, M., Fujioka, T., Machado, J. C. and Yamaoka, Y. (2008) Helicobacter and gastric malignancies. *Helicobacter* **1,** 28-34.
19. Bartnik, W. (2008) Clinical aspects of *Helicobacter pylori* infection. *Pol. Arch. Med. Wewn.* **118,** 426-430.
20. Covacci, A., Telford, J. L., Del Giudice, G., Parsonnet, J. and Rappuoli, R. (1999) *Helicobacter pylori* virulence and genetic geography. *Science* **284,** 1328-1333.
21. Tomb, J. F., White, O., Kerlavage, A. R., Clayton, R. A., Sutton, G. G., Fleischmann, R. D., Ketchum, K. A., Klenk, H. P., Gill, S., Dougherty, B. A., Nelson, K., Quackenbush, J., Zhou, L., Kirkness, E. F., Peterson, S., Loftus, B.,

Richardson, D., Dodson, R., Khalak, H. G., Glodek, A., McKenney, K., Fitzegerald, L. M., Lee, N., Adams, M. D., Hickey, E. K., Berg, D. E., Gocayne, J. D., Utterback, T. R., Peterson, J. D., Kelley, J. M., Cotton, M. D., Weidman, J. M., Fujii, C., Bowman, C., Watthey, L., Wallin, E., Hayes, W. S., Borodovsky, M., Karp, P. D., Smith, H. O., Fraser, C. M. and Venter, J. C. (1997) The complete genome sequence of the gastric pathogen *Helicobacter pylori*. *Nature* **388,** 539-547.

22. Alm, R. A., Ling, L. S., Moir, D. T., King, B. L., Brown, E. D., Doig, P. C., Smith, D. R., Noonan, B., Guild, B. C., deJonge, B. L., Carmel, G., Tummino, P. J., Caruso, A., Uria-Nickelsen, M., Mills, D. M., Ives, C., Gibson, R., Merberg, D., Mills, S. D., Jiang, Q., Taylor, D. E., Vovis, G. F. and Trust, T. J. (1999) Genomic-sequence comparison of two unrelated isolates of the human gastric pathogen *Helicobacter pylori*. *Nature* **397,** 176-180.
23. Oh, J. D., Kling-Bäckhed, H., Giannakis, M., Xu, J., Fulton, R. S., Fulton, L. A., Cordum, H. S., Wang, C., Elliott, G., Edwards, J., Mardis, E. R., Engstrand, L. G. and Gordon, J. I. (2006) The complete genome sequence of a chronic atrophic gastritis *Helicobacter pylori* strain: evolution during disease progression. *Proc. Natl. Acad. Sci. U.S.A.* **103,** 9999-10004.
24. Han, K.-D., Park S.-J., Jang, S.-B. and Lee, B.-J. (2008) Backbone ^{1}H, ^{15}N, and ^{13}C resonance assignments and secondary-structure of the conserved hypothetical protein HP0892 of *Helicobacter pylori*. *Mol. Cells* **25,** 138-141.
25. Seo, M.-D., Park, S.-J., Kim, H.-J., Seok, S.-H. and Lee, B.-J. (2007) Backbone ^{1}H, ^{15}N, and ^{13}C resonance assignment and secondary structure prediction of HP0495 from *Helicobacter pylori*. *J. Biochem. Mol. Biol.* **40,** 839-843.
26. Tsai, J. Y., Chen, B. T., Cheng, H. C., Chen, H. Y., Hsaio, N. W., Lyu, P. C. and Sun, Y. J. (2006) Crystal structure of HP0242, a hypothetical protein from *Helicobacter pylori* with a novel fold. *Proteins* **4,** 1138-1143.
27. Lüthy, L., Grütter, M. G. and Mittl, P. R. (2002) The crystal structure of *Helicobacter pylori* cysteine-rich protein B reveals a novel fold for a penicillin-binding protein. *J. Biol. Chem.* **277,** 10187-10193.
28. Hung, C. L., Liu, J. H., Chiu, W. C., Huang, S. W., Hwang, J. K. and Wang, W. C. (2007) Crystal structure of *Helicobacter pylori* formamidase AmiF reveals a cysteine-glutamate-lysine catalytic triad. *J. Biol. Chem.* **16,** 12220-12229.
29. Kim, N. Y., Weeks, D. L., Shin, J. M., David, R. S., Young, M. K. and Sachs, H. (2002) Proteins released by *Helicobacter pylori* in vitro. *J. Bacteriol.* **184,** 6155-6162.
30. Nam, W. H., Lee, S. M., Kim, E. S., Kim, J. H. and Jeong, J. Y. (2007) Mechanism of metronidazole resistance regulated by the *fdx*A gene in *Helicobacter pylori*. *J. Life Sci.* **17,** 723-727.
31. Mukhopadhyay, A. K., Jeong, J. Y., Dailidiene, D., Hoffman, P. S. and Berg, D. E. (2003) The fdxA ferredoxin gene can down-regulate frxA nitroreductase gene expression and is essential in many strains of *Helicobacter pylori*. *J. Bacteriol.* **185,** 2927-2935.
32. Dunwell, J. M., Purvis, A. and Khuri, S. (2004) Cupins: the most functionally diverse protein superfamily? *Phytochemistry* **65,** 7-17.
33. Mills, E. N. C., Jenkins, J., Marigheto, N., Belton, P. S., Gunning, A. P. and Morris, V. J. (2002) Allergens of the cupin superfamily. *Biochem. Soc. Trans.* **30,** 925-929.
34. Dunwell, J. M., Khuri, S. and Gane, P. J. (2000) Microbial relatives of the seed storage proteins of higher plants: conservation of structure and diversification of function during evolution of the cupin superfamily. *Microbiol. Mol. Biol. Rev.* **64,** 153-179.
35. Lee, C.-J., Won, H.-S., Kim, J.-M., Lee, B.-J. and Kang, S.-O. (2007) Molecular domain organization of BldD, an essential transcriptional regulator for developmental process of *Streptomyces coelicolor* A3(2). *Proteins* **68,** 344-352.
36. Won, H.-S., Seo, M.-D., Ko, H.- S., Choi, W.-S. and Lee, B.-J. (2008) Thermal denaturation of the apo-cyclic AMP receptor protein and noncovalent interactions between its domains. *Mol. Cells* **26,** 61-66.
37. Lee, Y.-H., Won, H.-S., Lee, M.-H. and Lee, B.-J. (2002) Effects of salt and nickel ion on the conformational stability of *Bacillus pasteurii* UreE. *FEBS Lett.* **522,** 135-140.
38. Delaglio, F., Grzesiek, S., Vuister, G. W., Zhu, G., Pfeifer, J. and Bax, A. (1995) NMRPipe: a multidimensional spectral processing system based on UNIX pipes. *J. Biomol. NMR* **6,** 277-293.
39. Johnson, B. A. (2004) Using NMRView to visualize and analyze the NMR spectra of macromolecules. *Methods Mol. Biol.* **278,** 313-352.
40. Won, H.-S., Yamazaki, T., Lee, T.-W., Jee, J.-G., Yoon, M.-K., Park, S.-H., Otomo, T., Aiba, H., Kyogoku, Y. and Lee, B.-J. (2000) Backbone NMR assignments of a high molecular weight protein (47 kDa), cyclic AMP receptor protein (apo-CRP). *J. Biomol. NMR* **16,** 79-80.
41. Lee, Y.-H., Won, H.-S., Ahn, H.-C., Park, S.-H., Yagi, H., Akutsu, H. and Lee, B.-J. (2000) Backbone NMR assignments of the metal-free UreE from *Bacillus pasteurii*. *J. Biomol. NMR* **24,** 361-362.
42. Won, H.-S., Yamazaki, T., Lee, T.-W., Yoon, M.-K., Park, S.-H., Kyogoku, Y. and Lee, B.-J. (2000) Structural understanding of the allosteric conformational change of cyclic AMP receptor protein by cyclic AMP binding. *Biochemistry* **39,** 13953-13962.